Journal of Marine Science and Technology, Vol. 26, No. 4, pp. 496-507 (2018)
DOI: 10.6119/JMST.201808_26(4).0003

DESIGN OF A TWO-BODY WAVE ENERGY CONVERTER BY INCORPORATING THE EFFECT OF HYDRAULIC POWER TAKE-OFF PARAMETERS

Mohammadreza Negahdari, Hossein Dalayeli, and Mohammad Hassan Moghadas

Key words: wave energy converter (WEC), floating-point absorber (FPA), power take off (PTO), response amplitude operator (RAO).

ABSTRACT

Today, more than 80% of world's energy is obtained from the fossil fuels. Therefore, the researchers are looking for new methods for exploitation of renewable energy resources. Sea waves are an important source of environmental energy which can be converted into energy needed for different purposes. In current study, a floating-point absorber wave energy converter is simulated and optimized by the authors. The system is modeled through a two-body floating-point absorber (FPA) with two degrees of freedom in the heave direction. The model is equipped with a hydraulic power take off (PTO) system aiming to study the performance of the two-body wave energy converter (WEC) in regular and irregular waves. The fluid and structural parameters of the point absorber have been calculated and used for the purpose of optimization. Then, the optimum PTO damping coefficient was obtained and applied to this optimum value for system modeling. Further, a simulation study was performed in order to analyze the hydrodynamics of the two-body FPA system and its power output in the actual operational wave climate. Therefore, this paper has illustrated the application of a hydraulic power take off (PTO) system, giving an integrated pattern for modeling and designing of a wave energy converter system which is based on the hydrodynamic, hydraulic and structural dynamic fields. The results indicated that this modified system is optimal.

Paper submitted 11/16/17; revised 01/24/18; accepted 05/22/18. Author for correspondence: Mohammad Reza Negahdari (e-mail address: m.r.negahdari@gmail.com).
Department of Mechanical Engineering, Malek Ashtar University Of Technology University, Esfahan, Iran.

I. INTRODUCTION

A growing need for energy and high costs of energy production in all industries have led human to make use of natural energy resources. Sea waves have been considered as an important source of energy and a wide range of studies have been conducted in all aspects of this energy resource. Waves are generated by the effects of wind on the sea surface. Point absorbers are floating wave energy converters (WEC's) whose dimensions are much smaller than the wavelength. They oscillate with the ocean waves with one or more degrees of freedom. A point absorber is capable of absorbing wave energy from a wave front which is greater than the physical dimensions of the device itself (Faizal et al., 2014). Therefore, this device is one of the most popular invented designs which has been considered as one of the most promising and cost-effective energy producing devices in the world.

Today, some parts of the electricity consumed in the island of Madeira, Portugal, and Greek Island are produced through the wave energy converters floating-point absorber; in addition, in Ireland and the island of Azores, Portugal, the SEAREV and OPT point absorber systems are being employed (Nazari et al., 2013). Regarding this issue, different studies have been conducted in the field of floating-point absorber wave energy converters. Koh et al. (2013) studied the effects of resonance on the energy absorbed by the point absorber. In the same vein, Pastor and Liu (2014) investigated the wave energy absorption in different forms of buoys. In addition, the floating-point absorber wave energy converter was presented by Li and Yu (2013) based on the model of OPT-PB150. Bozzi et al. (2013) investigated the impacts of using a system consisting of two bodies which are the floating and submerged ones. Moreover, he considered the effects of these bodies' dimensions on the output power as well. Furthermore, another research showed that the absorption power of the two-body systems can be significantly higher than the single body systems with the same floating (Liang and Zuo, 2017). The results indicated that the output power could be considerably increased if the floating body was connected to a submerged body. Amiri et al. (2016) investigated the effects of wave characteristics on the energy conversion and device efficiency which include wave height, wave period, buoy geometry, and damping coefficient for a two-body floating-point absorber. More recent studies have focused on improving the wave absorption efficiency of wave energy converters.

Since the amount of wave energy extraction technologies is consistent with climate conditions and specifications governing the sea waves of Iran, it is suggested that application of the floating-point absorbers could be the best option in Iran (Alamian et al., 2014). Therefore, the current study aimed to do some modification on the FPA system in order to reach maximum optimization. The proposed two-body FPA model has two components, including the floating and fully submerged bodies and these two are connected through a mass-spring-damper system. For this purpose, the spring was utilized solely to connect the two sections. Then, a damper was used to represent the PTO mechanism which is used for energy transfer between waves and converters. Energy absorption method by the converter is due to vertical movements in waves. In other words, the up and down vertical movements of the bodies can be exploited to transfer and convert wave energy into mechanical energy. The energy is extracted through the relative heave motion of the floating and submerged oscillating bodies. Studies on the optimal control strategy showed that the heave response and converted power of a heaving WEC had a significant increase through the hydraulic power take off system (Yu and Li, 2011). This system offers the advantage of storing large quantities of energy through the accumulators. The theory of linear oscillations states that for optimal power absorption, wave energy devices should operate close to their resonance condition, where the PTO damping coefficient of the system is determined to maximize the power absorption by achieving resonance and an optimal value of damping.

As shown in Fig. 1, the FPA model was used in this study. This model was utilized because it represents the point absorbers designs currently being developed. Furthermore, this model has experimental data which is derived from wave tank testing. The experimental data was used to validate the results presented in this paper. Furthermore, the geometry and the dimension of two FPA models were shown in Fig. 1. The single-body point absorber is modeled as one rigid body, which is shown on the left side of Fig. 1. The single body system assumes that the absorber is locked, and the device is moved as a rigid body. Here, we only considered a basic structural design but the effects of mooring lines were ignored. The mass of the full-scale single body model was approximately 249 metric tons with the center of gravity situated 22.4 m below the mean of free surface. The floating and the submerged bodies weighed 84.5 metric tons and 165 metric tons respectively. The optimal values of the PTO coefficients can be used in the hydraulic system. In other words, after determining the optimal coefficients of the proposed equations, conditions for realizing these coefficients in the hydraulic system are determined and applied. The findings show that, the hydraulic motor and generator damping have the greatest effect on the damping coefficient (c_{pto}); moreover, the stiffness coefficient value (k_{pto}) is influenced by the hydraulic cylinder and accumulators specifications. For this purpose, the values of the hydraulic parameters of the system are determined so that the hydraulic system reaches resonance conditions and the power of the system will be maximized accordingly. In this paper, an integrated pattern for modeling and designing of wave energy converter system is presented based on hydrodynamic, hydraulic and structural dynamic fields.

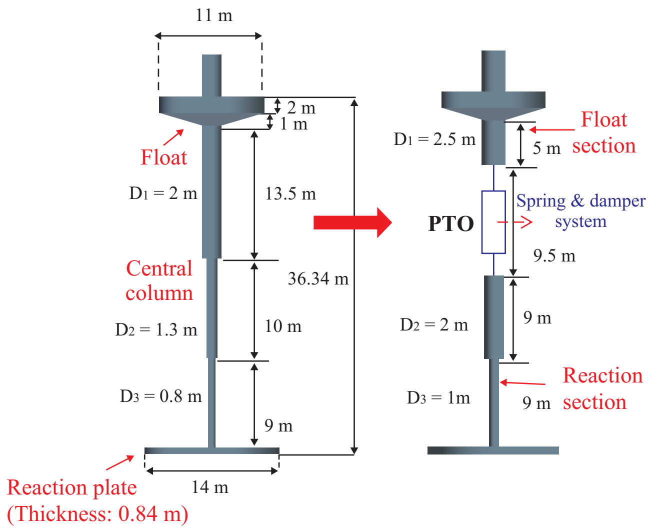

Fig. 1. Two-Body Floating Point Absorber (Yu and Lie, 2011).

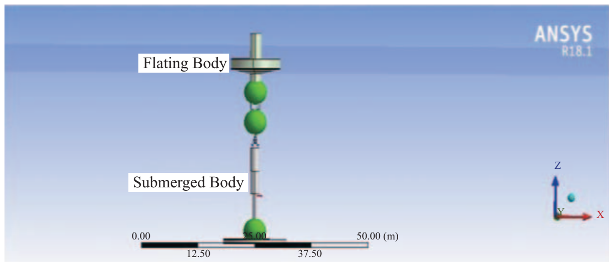

Fig. 2. FPA model used in AQWA simulation.

In section 2, the calculation of hydrodynamic coefficients of a two body wave energy converter is established under regular wave excitation. For system modeling, the boundary element method software, ANSYS AQWA, was used in order to perform a hydrodynamic analysis. The equations needed to determine the optimum power and the closed form solution of absorption are obtained in section 3. In section 4, the hydraulic system modeling and optimum power take-off design and the corresponding absorption power are taken into account. Results and conclusions are given in section 5 and 6, respectively.

II. MODELING AND THE CALCULATION OF HYDRODYNAMIC COEFFICIENTS

In this section, the calculation of hydrodynamic coefficients in the equations of motion for the system has been studied. The study was carried out in order to achieve optimal model. Modeling hydrodynamic system has been done in ANSYS-AQWA soft-

Table 1. Two-Body Point Absorber Dimensions.

Floating	Diameter	11 m
	Height	3 m
Spar	Diameter	2 m
	Height	36.34 m
Submerged	Diameter	14 m
	Height	0.84 m

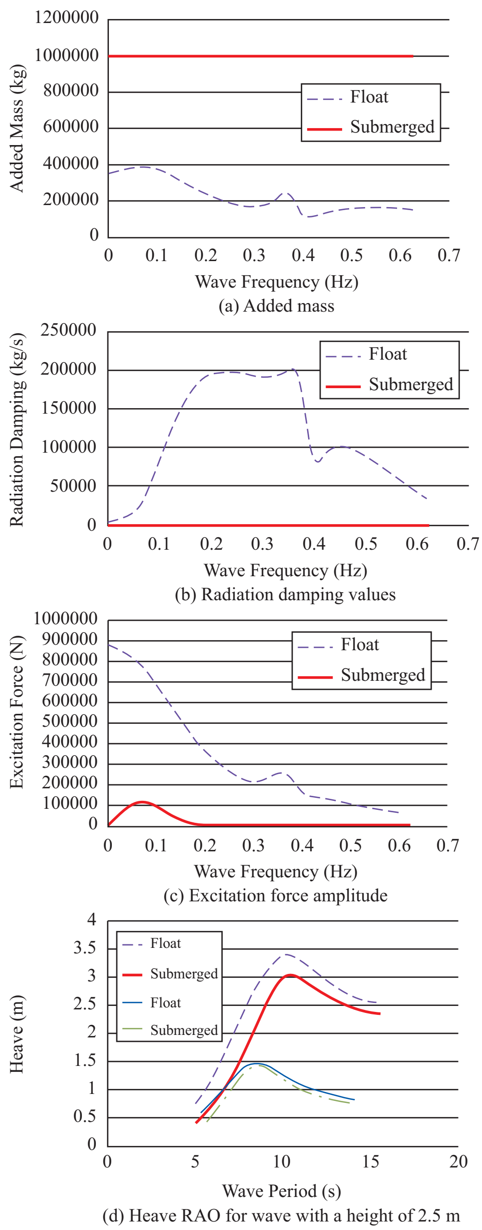

Fig. 3. Hydrodynamic parameters of the two buoy configurations.

ware. AQWA is a BEM code based on the principles of linear wave theory, so the frequency-domain response has the assumptions of incompressible, irrotational, and inviscid flow. The two-body point absorber was modeled in AQWA. The 3D geometry

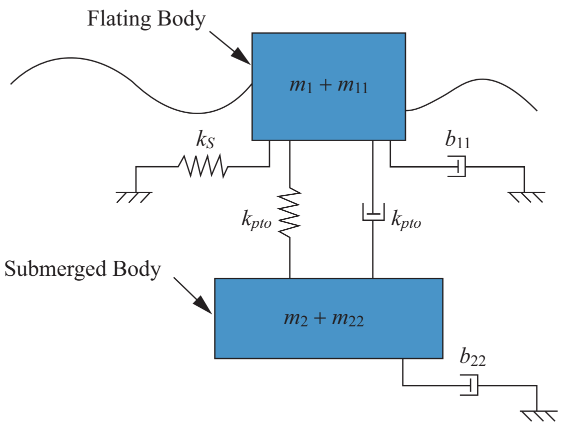

Fig. 4. Free-body diagram of two body system.

of the two-body point absorber is shown in Fig. 2, and their dimensions are given in Table 1.

Fig. 3 shows the hydrodynamic results of the system in the frequency-domain. ANSYS AQWA was used to obtain the results. Added mass values for different frequencies are given in Fig. 3(a), and radiation damping values and excitation force amplitude for each body are shown in Figs. 3(b) and 3(c), respectively. In Fig. 3(d), heave RAO and added mass values for different frequencies are shown, RAO analysis can extract frequencies where maximum power is determined. As can be seen in Fig. 3(d), the heave response of the floating and the submerged bodies, where the values were plotted against the wave period are presented. The relative motion between the two bodies, had a peak periods of around $T = 8$ s. To ensure the accuracy of results, we compared the different wave periods obtained from numerical results with those in the experimental data. In December 2010, an experimental test was performed at UC Berkeley's wave tank to validate the numerical prediction (Yu and Li, 2013).

To achieve the maximum output power, the frequency of the system was considered equal to the wave frequency. The wave frequency is the dominant frequency of the waves, which equals to 0.125 Hz in this analysis.

III. MAIN GOVERNING EQUATIONS

In this section, the equations for determining the optimum power will be presented in order to perform system optimization process. Fig. 4 shows the free body diagram of the two-body wave energy converter. A floating buoy is located on the water surface and is connected to a submerged body through a power take-off (PTO) system.

The proposed equations include the governing equations of the system. These equations include the following relationships (Kassem et al., 2015):

$$\begin{aligned} F_{e1} - F_{r11} - F_{r12} - F_{PTO} &= \rho g A_1 z_1 + (M_1 + m_1)\ddot{z}_1 \\ F_{e2} - F_{r22} - F_{r21} + F_{PTO} &= (M_2 + m_2)\ddot{z}_2 \end{aligned} \quad (1)$$

The above equations are equations of motion for the two degrees of freedom, where, z_1 and z_2 are the heave displacements of the floating and submerged bodies. M_1 and M_2 are the respective masses of the floating and submerged bodies. A_1 is the water plane surface area of the floating body. F_{e1} and F_{e2} are the amplitudes of the wave excitation forces on the two bodies. The exciting force can be defined as a harmonic function in regular waves with the following equation:

$$F_{e1} = F_1 e^{i\omega t}, F_{e2} = F_2 e^{i\omega t} \tag{2}$$

and radiation forces F_{ri} and coupling radiation force F_{r12}, F_{r21} are given in Eq. (3):

$$\begin{aligned} F_{r11} &= A_{11}\ddot{z}_1 + b_1\dot{z}_1 \\ F_{r22} &= A_{22}\ddot{z}_2 + b_2\dot{z}_2 \\ F_{r12} &= A_{12}\ddot{z}_2 \\ F_{r21} &= A_{21}\ddot{z}_1 \end{aligned} \tag{3}$$

A_{ij} (i = 1, 2, j = 1, 2) are the elements of the added mass matrix which are calculated for the mass of the water moving with the i-th body induced by the motion of j-th body. The subscript 1 is denoted to the floating body and the subscript 2 is denoted to the submerged body. By substituting different terms, relations can be rewritten as follows:

$$\begin{aligned} &m_1\ddot{z}_1 + b_1\dot{z}_1 + A_{11}\ddot{z}_1 + A_{12}\ddot{z}_2 + c_{pto}(\dot{z}_1 - \dot{z}_2) + k_{pto}(z_1 - z_2) + \rho g A_1 z_1 = F_{e1} \\ &m_2\ddot{z}_2 + b_2\dot{z}_2 + A_{11}\ddot{z}_1 + A_{21}\ddot{z}_1 - c_{pto}(\dot{z}_1 - \dot{z}_2) - k_{pto}(z_1 - z_2) = F_{e2} \end{aligned} \tag{4}$$

where k_{pto} and c_{pto} are the stiffness and damping coefficients of the power take-off system and the PTO force is assumed to be linear as follow (Xie and Zuo, 2013):

$$F_{pto} = c_{pto}(\dot{z}_1 - \dot{z}_2) + k_{pto}(z_1 - z_2) \tag{5}$$

Then the average output power of a two-body wave energy converter is: (Falcao, 2010)

$$P_{ave} = \frac{1}{T}\int_0^T c_{pto}(\dot{z}_1 - \dot{z}_2)^2\, dt = \frac{1}{2}\omega^2 c_{pto}\left|Z_1 - Z_2\right|^2 \tag{6}$$

where Z_1 and Z_2 are the amplitudes of the velocity of floating body and submerged body, respectively. The closed-form solution of average output power (P_{ave}) can be expressed in the form of Eq. (7) (Liang and Zuo, 2017):

$$P_{ave} = \frac{1}{2}\omega^2 c_{pto}\left|\frac{p + iq}{(a + ib)c_{pto} + (c + id)k_{pto} + e + if}\right|^2 \tag{7}$$

where

$$\begin{cases} p = k_s F_2 - \omega^2(m_2 + A_{22} + A_{21})F_1 - \omega^2(m_1 + A_{11} + A_{12})F_2 \\ q = \omega(b_{22} + b_{vis\_2} + b_{21})F_1 + \omega(b_{11} + b_{vis\_1} + b_{12})F_2 \\ a = -\omega^2(b_{11} + b_{vis\_1} + b_{22} + b_{vis\_2} + b_{12} + b_{21}) \\ b = \omega k_s - \omega^3\left[(m_1 + A_{11}) + (m_2 + A_{22}) + A_{12} + A_{12})\right] \\ c = b/\omega \\ d = -a/\omega \\ e = \omega^4\left[(m_1 + A_{11})(m_2 + A_{22}) - A_{12}A_{21})\right] \\ \quad - \omega^2(m_2 + A_{22})k_s + (b_{11} + b_{vis\_1})(b_{22} + b_{vis\_2}) - b_{12}b_{21} \\ f = -\omega^3[(m_1 + A_{11})(b_{22} + b_{vis\_2}) + (m_2 + A_{22})(b_{11} + b_{vis\_1}) \\ \quad - A_{12}b_{12} - A_{21}b_{21}] + \omega k_s(b_{22} + b_{vis\_2}) \end{cases}$$

As a result, the values of added mass (m_{12}, m_{21}) and radiation damping (b_{12}, b_{21}) can be neglected. By taking the partial derivative of Eq. (7) with respect to k_{pto} and c_{pto}, respectively, the optimal conditions of these parameters are obtained as,

$$(k_{pto})_{opt} = -\frac{ce + df}{c^2 + d^2} \tag{8}$$

$$(c_{pto})_{opt} = \frac{1}{\omega}\frac{\left|cf - de\right|}{c^2 + d^2} \tag{9}$$

Hence, by substituting k_{pto} of Eq. (8) and c_{pto} of Eq. (9) into Eq. (7), the optimum power can be found as:

$$(P_{ave})_{opt} = \frac{1}{2}\omega^2\frac{p^2 + q^2}{2\left|ae + bf\right| + 2(ae + bf)} \tag{10}$$

Eqs. (8)-(10) are called optimal condition of a two body wave energy converter (Liang and Zuo, 2017).

IV. HYDRAULIC SYSTEM MODELLING

This work considers a heaving point absorber with a hydraulic power take off unit. A hydrodynamic and hydraulic models were developed by using the Simulink and Simhydraulics software package. The optimal value of PTO damping is considered to maximize power generation which is related to the wave frequency and the velocity of the system. Hydraulic PTOs are generally used in WECs due to their ability to deal with low frequency, high force wave inputs and their high power density and robustness. Schematic of the hydraulic PTO system used in this simulation is shown in Fig. 5.

Two other equations are related to PTO hydraulic power system consisting input power and generated power respectively, which can be expressed as follows:

$$P_{gen} = T_g \cdot \omega_m \tag{11}$$

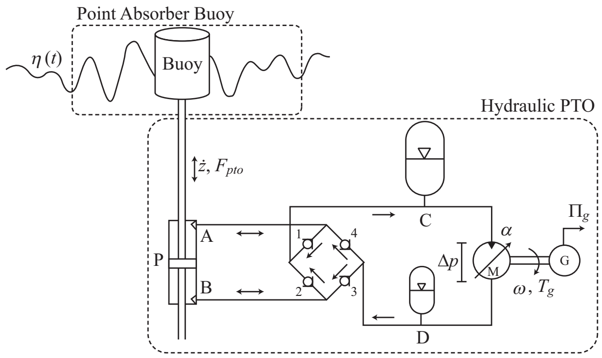

Fig. 5. Schematic of the hydraulic PTO system (Casey, 2014).

$$P_{ave} = \frac{1}{T}\int_0^T c_{pto}(\dot{z}_1 - \dot{z}_2)^2 dt \tag{12}$$

And the generator torque is given by (Casey, 2014)

$$T_g = C_g \cdot \omega_m \tag{13}$$

where ω_m is the motor speed and C_g is the generator damping coefficient. The PTO damping was optimized for energy absorption by adjusting the motor displacement. To maximize the power generated, the effective PTO damping term (α) was formulated as (Cargo, 2012):

$$\alpha = (\frac{A_p}{D_m})^2 \cdot C_g \tag{14}$$

Where A_p is the piston area and D_m is the motor displacement. The value of C_g determines with respect to PTO damping coefficient. The value of PTO damping, which can be expressed as follows:

$$C_{pto} = \alpha + C_{pressure-drop} + C_{cylinder} \tag{15}$$

where $C_{cylinder}$ is the damping coefficient of hydraulic cylinder and $C_{pressure\text{-}drop}$ is the average damping coefficient of pressure drop in hydraulic system. The average damping coefficient of pressure drop is obtained as:

$$C_{pressure-drop})_{ave} = \frac{Q.\Delta P}{V_{rel}^2} \tag{16}$$

where Q is fluid flow rates, ΔP is pressure drop and V_{rel} is piston velocity which was obtained from relative velocity between floating and submerged bodies. The value of Stiffness coefficient of PTO system (K_{pto}) in hydraulic system can be expressed as follows:

Table 2. Results of the system modeling in two degree of freedom (*T* = 8 s).

Parameter	Type	Values
m_1 (kg)	Floating mass	84500
m_2 (kg)	submerged body mass	165000
m_{11} (kg)	Added mass of floating	437500
m_{22} (kg)	Added mass of submerged	1013000
b_1 (Ns/m)	Damping coefficient of floating	100000
b_2 (Ns/m)	Damping coefficient of submerged	4000
F_{e1} (N)	The wave excitation of floating	900000
F_{e2} (N)	The wave excitation of submerged	2000

Table 3. Results of the optimal PTO coefficients and optimum power of the system (*T* = 8s).

Parameter	Type	Values
$c_{pto)opt}$ (kNs/m)	Damping coefficient of PTO system	1200
$k_{pto)opt}$ (kN/m)	Stiffness coefficient of PTO system	20
P_{ave} (kw)	Average power output	131

$$K_s = \frac{dF}{dx} \tag{17}$$

$$K_{pto} = \frac{d\left[A_p(P_H - P_L)\right]}{dx} \tag{18}$$

where P_H and P_L are the high and low pressure accumulators, respectively. The pressure in the accumulators during the up and down stroke can be changed with piston displacement changes (dx).

V. RESULTS AND DISCUSSION

1. Hydrodynamic & Hydraulic Parameters

Simulation of a two-body WEC was performed with regular wave inputs. The results are presented for the period of 8 s in Table 2. Table 3 shows the optimal conditions consisting of PTO coefficient and optimum power obtained from Eqs. (8)-(10). From this table, the optimum value for the damping coefficient of the PTO mechanism, c_{pto}, at the point where the total mean absorbed power is at its maximum value, was determined as 1200 kNs/m.

Then the governing equations of the system were solved and the system velocity values were calculated. For this purpose, the optimal power take off coefficient was employed. Fig. 6 shows the velocity responses of the floating body and submerged body, respectively.

The natural frequencies, ω_n, of the system were calculated. They may be calculated by the assumption that the system is undamped. The damped natural frequencies are as follows:

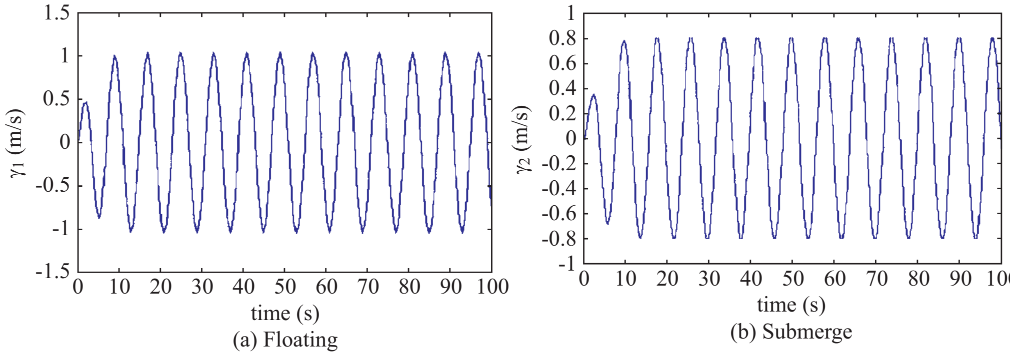

Fig. 6. Velocities for heave directions of Two-Body FPA.

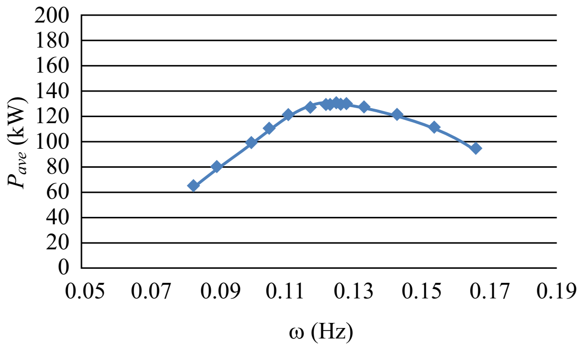

Fig. 7. Average power from the hydrodynamic analysis.

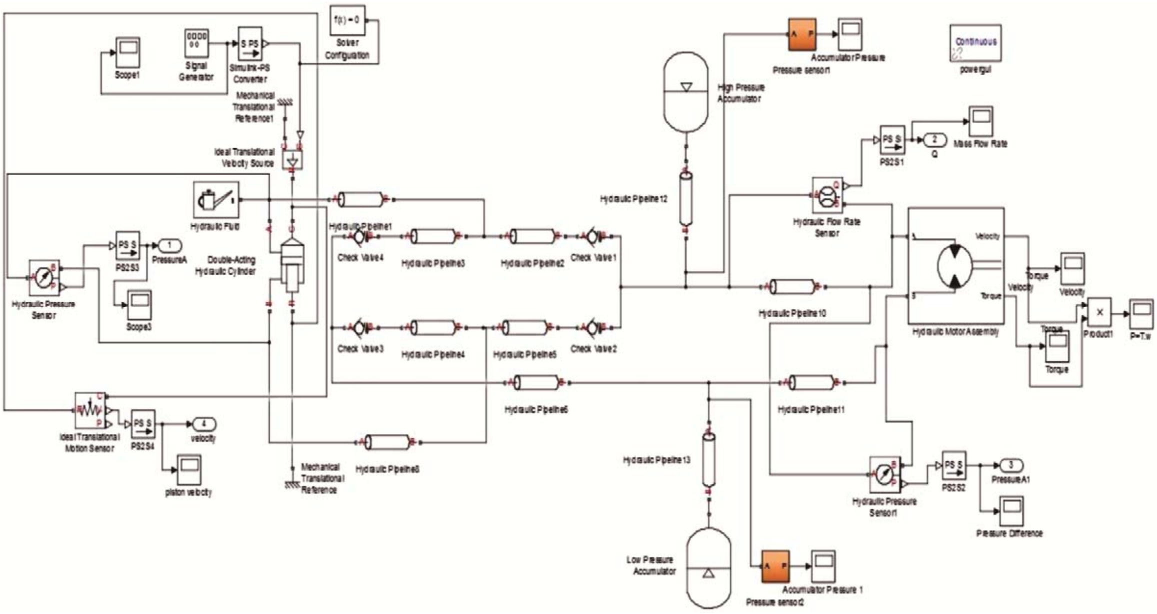

Fig. 8. Simulation of Hydraulic circuit system.

$\omega_d = \omega_n \sqrt{1-\zeta^2}$, where the damping frequency is always less than, or equal to the corresponding undamped frequency. (Finnegan, 2012). The values of these frequencies for two bodies of FPA system were calculated. From this analysis it can be concluded that this system has 2 frequencies which only one of them is equal to frequency of the wave. Using the submerged body causes one of the frequencies to approach the frequency of the wave. The results showed that 0.125 Hz was the fre-

Table 4. Simulation parameters used for the hydraulic PTO system.

	Values
Maximum system pressure	450 bar
Piston area (A_P)	0.01 m^2
Motor displacement (D_m)	0.0000132 m^3/rev
HP Accumulator volume	7 m^3
HP Acc. Pre-charge pressure	40 bar
LP Accumulator volume	3 m^3
LP Acc. Pre-charge pressure	20 bar
Maximum valve area	0.0001 m^2
Discharge coefficient	0.5
Generator damping	5.21 N · m/(rad/s)
Oil properties, viscosity	35 cSt
Oil properties, density	850 kg/m^3

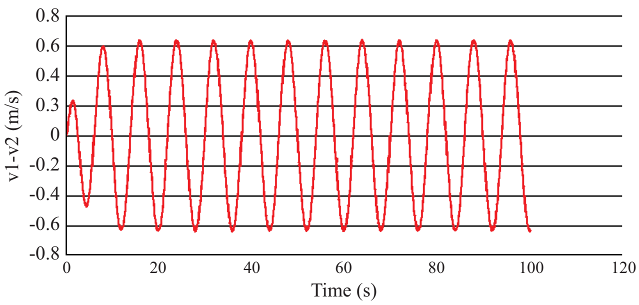

Fig. 9. Relative velocity of piston.

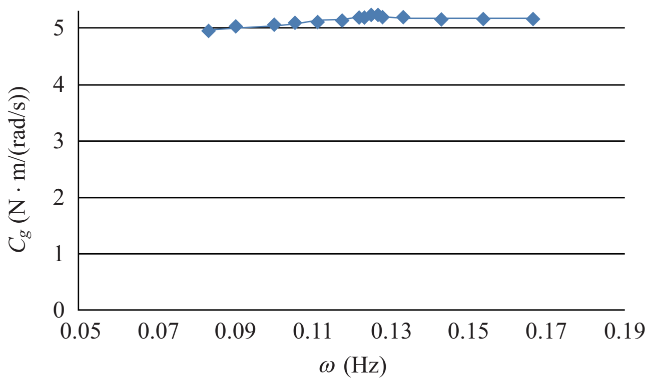

Fig. 11. Generator damping values.

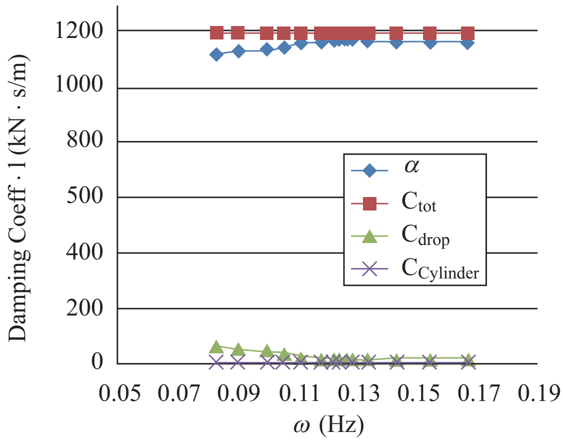

Fig. 10. Damping values of hydraulic system.

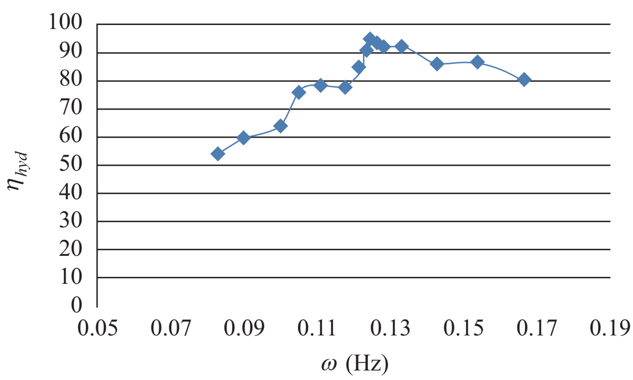

Fig. 12. Hydraulic system efficiency.

quency of the system. This value is equal to the dominant frequency of the sea waves and it causes resonance condition. Fig. 7 represents the average power obtained from the hydrodynamic analysis of the system. This graph shows that the maximum power has occurred at the resonant frequency of 0.125 Hz.

Fig. 8 depicts the simulation of Hydraulic circuit system. Fig. 9, shows the piston velocity which was obtained from the relative velocity between floating and submerged bodies.

Damping values for various frequencies were calculated and presented in Fig. 10, by analysis of the hydraulic circuit and considering the damping action in the cylinder and the system pressure drop. According to Eq. (14), the generator

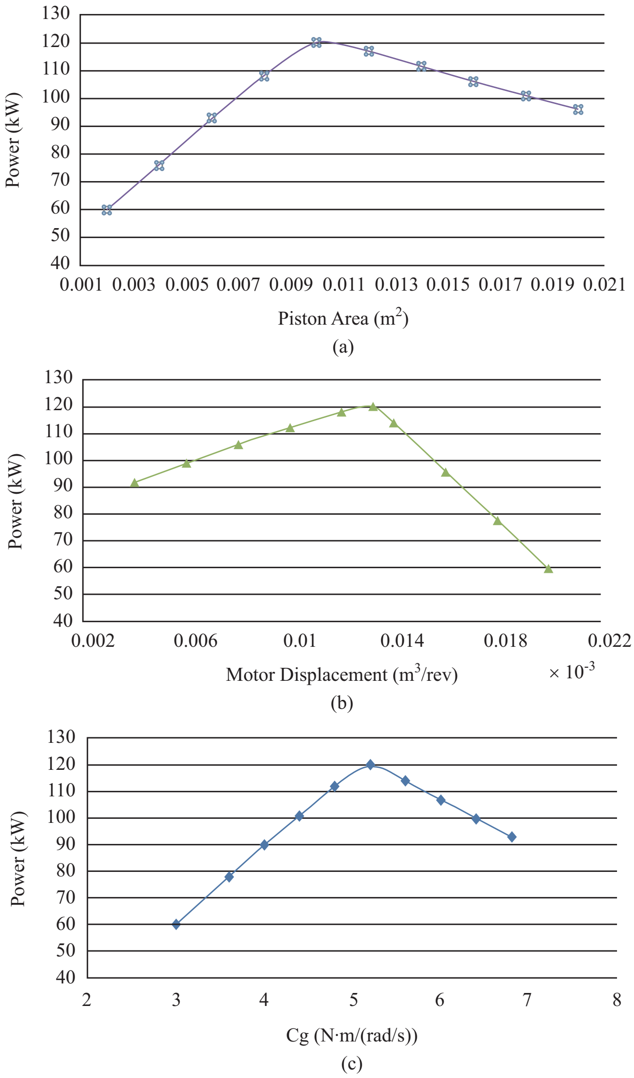

Fig. 13. Power absorption vs. (a) piston area, (b) motor displacement and (c) generator damping coefficient.

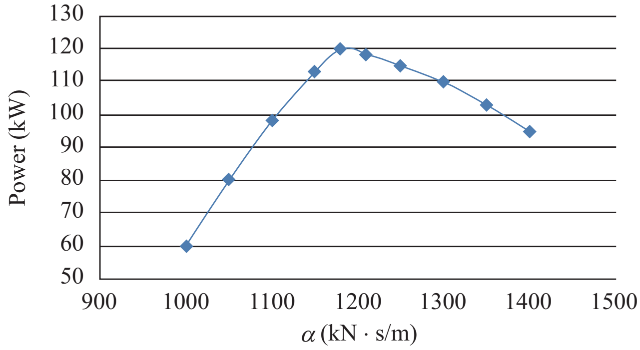

Fig. 14. Power absorption vs. PTO damping coefficient.

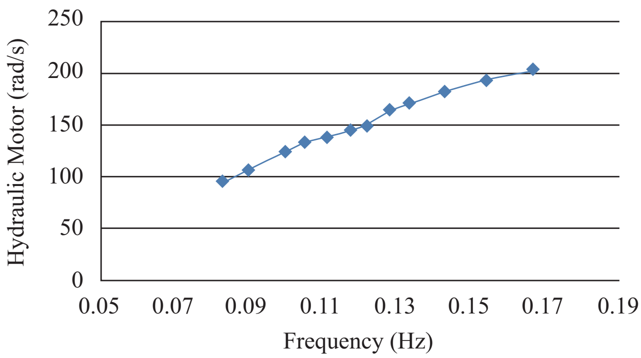

Fig. 15. Hydraulic motor speed vs. wave frequency.

damping values (C_g) were obtained at various frequencies and illustrated as the graph in Fig. 11. As shown in this graph, the generator damping coefficient at the frequency of 0.125 Hz was maximum and equal to 5.21 N · m/(rad/s). Table 4 shows the numerical results of the hydraulic parameters obtained from the system analysis. Based on the Eqs. (17) and (18), the value of stiffness coefficient of PTO system (K_{pto}) in hydraulic system was calculated. The average PTO stiffness coefficient was approximately equal to 20 kN/m.

The hydraulic system efficiency values at various frequencies are shown in Fig. 12. This graph also shows that the maximum power has occurred at the resonant frequency of 0.125 Hz ($T = 8$ s).

2. Maximizing Power Absorption in the Hydraulic PTO System

This section discusses the ways to maximize power absorption in the hydraulic PTO system. In the previous section, the values of the optimal PTO damping and maximum power capture were obtained and it was shown that the hydraulic PTO system could be tuned by knowing the wave frequency.

Results verify that the power absorption can be maximized by changing the PTO damping and providing optimal values for the system. According to Eq. (14), the damping term for the hy-draulic PTO system was derived from the relationship between the piston area, motor displacement, and generator damping. The three components are effective in the power absorption. Each of the mentioned components varied independently, to give the same values of PTO damping. This suggests that the PTO can be tuned by changing any of these three components to alter α. By using this method, the PTO damping for maximizing wave energy conversion should always be set to the suitable values of these components (Cargo, 2012). The simulations have been applied with a regular wave of $H = 2.5$ m and $T = 8$ s. The effects of the three components on power is shown in Fig. 13. Fig. 14 shows that the power absorption can be maximized by varying α.

in fact, the frequency can be shifted according to the configuration variations. For this reason, the motor displacement will be varied because in practice only this component can be easily changed. To ensure that the power absorption remains at its maximum, α must be maintained constant during controlling the hydraulic motor speed (Cargo, 2012). To maintain the required motor speed, motor displacement is continuously varying. How-

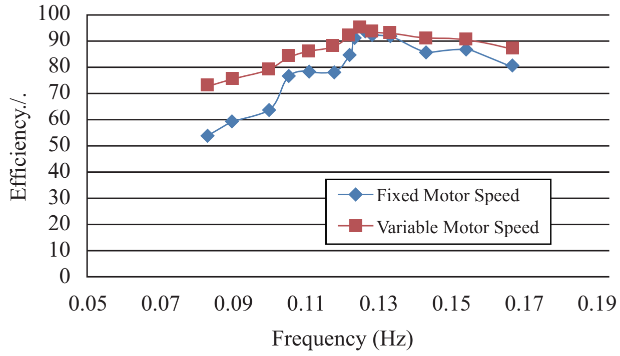

Fig. 16. Power absorption efficiency for PTO hydraulic system.

Table 5. Sea states values for Chabahar bay (Ports and Maritime Organization of Iran).

Sea states	H_S (m)	T_P (s)
1	0.25	6
2	0.75	6.5
3	1.5	7
4	2.5	8
5	3	9
6	3.75	10
7	5	11
8	6.5	12

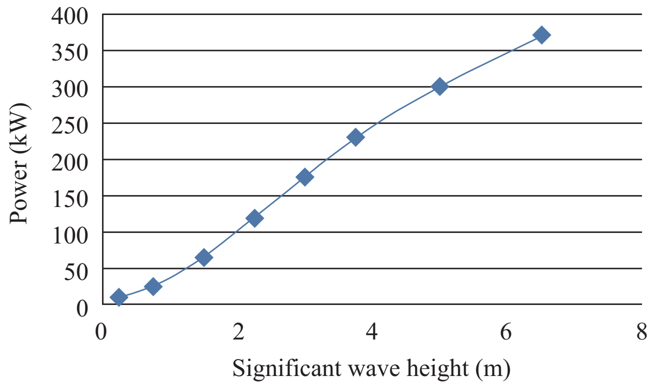

Fig. 17. Power absorption of the two-body system vs. significant wave height.

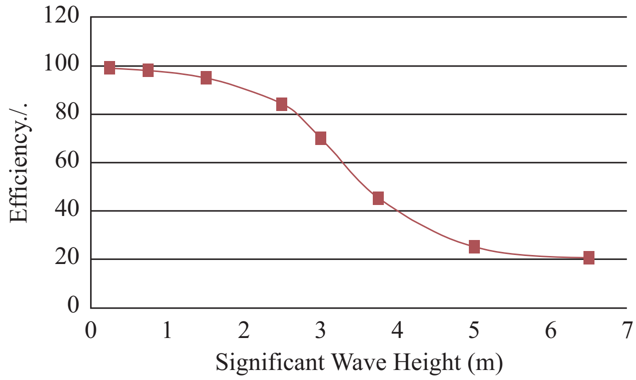

Fig. 18. Efficiency of the two-body system vs. significant wave height.

ever, the motor speed should be remained within the operational limits for the PTO system in different wave conditions. Fig. 15 displays the motor speed for the optimal PTO system.

Thus, the PTO efficiency can possibly be improved in different sea conditions by using a variable displacement hydraulic motor. The results show that by controlling the hydraulic motor speed within the limited range, a remarkable increase of the power absorption efficiency is achieved for different wave frequencies. As shown in Fig. 16, the improvement of efficiency is obvious for the hydraulic PTO system.

3. Wave Climate

According to previous studies, the point absorber systems are very effective to be applied in Iran seas (Alamian et al., 2014). The potential of wave energy extraction can be investigated through the analysis of wave climate.

Rashid and Hasanzadeh (2011) examined the possible examples of offshore wave power installations at Chabahar area in the Oman Sea. They pointed out that Chabahar bay should be recognized as a suitable area for installation of wave energy converters. In this study, the Chabahar area had been chosen to represent a range of offshore wave climates.

The two main characteristics used to describe the wave climate of a given location is the significant wave height, H_s, which is the average of 1/3 the highest of the wave height, and the peak period (T_P). The calculations of power absorption were performed for different sea states, as defined in Table 5.

The results of the simulation, including power absorption and absorption efficiency, were obtained as the functions of the significant wave height (H_s) and its associated peak wave period (T_P). These results are displayed in Figs. 17 and 18. Fig. 18 indicates that increasing the significant wave height will increase the power absorbed by the system.

The absorption efficiency is defined by the ratio between the average power and the incident wave power

$$\eta_{abs} = \frac{P_{ave}}{P_w} \quad (19)$$

Eq. (20) gives the wave power for a regular wave per unit crest width, under ideal conditions:

$$P_w = \frac{\rho g^2 H^2 T}{16\pi} \quad (\frac{kW}{m}) \quad (20)$$

The value of optimal PTO damping coefficient then remained constant during the course of the analysis while testing the ef-

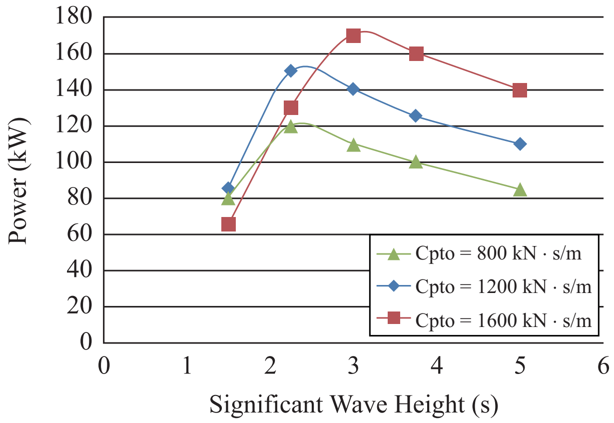

Fig. 19. Power absorption distribution vs. significant wave height.

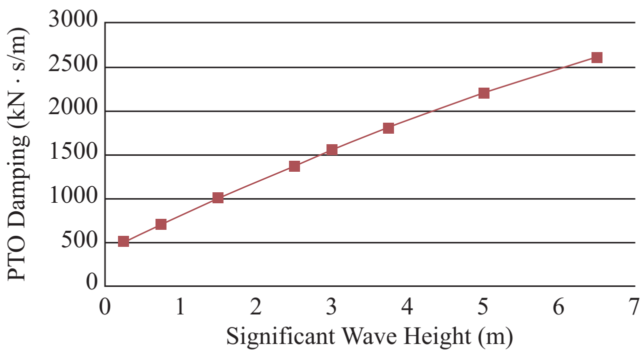

Fig. 20. Optimal PTO damping vs. significant wave height.

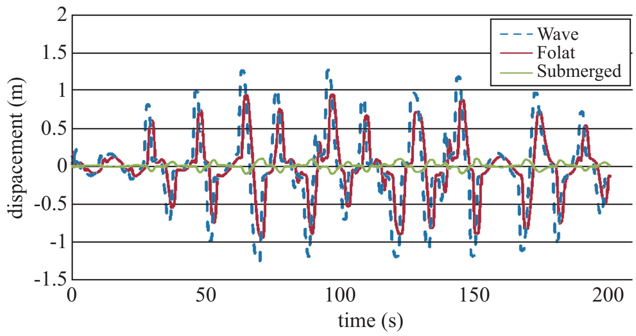

Fig. 21. Wave and WEC displacement (H_s = 2.5m and T_p = 8 s).

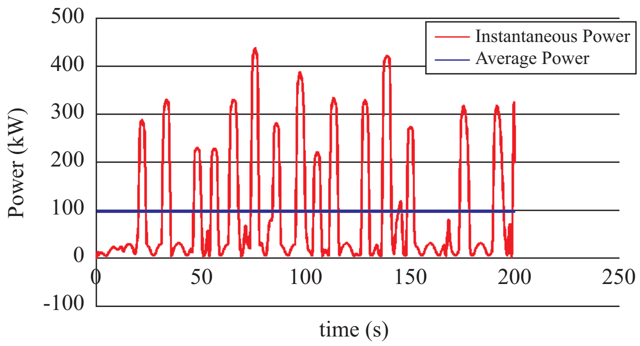

Fig. 22. Instantaneous and average power absorption by the two-body WEC system applying irregular waves.

ficiency throughout the remaining H_s and T_p values from Table 5.

Fig. 18 gives the conversion efficiency against the significant wave height for the two-body system. From this Figure, we will find that the efficiency of the system decreases when the significant wave height increases from 0.25 to 6.5.

Considering the PTO damping configuration, it can be seen that for the system, the optimal PTO damping values in a wave climate are different from the values for regular waves. Fig. 19 gives the average power absorption against the significant wave height with PTO damping of 800, 1200, and 1600 kN · s/m for the system located at the Bay of Chabahar.

4. Power Absorption in Irregular Waves

Real seas are not regular, so it is necessary to predict how WECs will behave in irregular wave conditions. An irregular wave can be obtained by superimposing several sinusoids of different heights and periods. The wave amplitude of each component is derived from the wave spectrum. Various spectra have been created using practical data to approximate different sea states. In this study, the generated spectrum based on a parameterized JONSWAP spectrum was used to model the irregular waves. The formula of the JONSWAP spectrum is expressed as (Kalofotias, 2016):

$$S_\zeta(\omega) = 320\frac{H_s^2}{T_p^4}\omega^{-5}\exp\left(\frac{-1950}{T_p^4}\omega^{-4}\right)\gamma^A$$

$$A = \exp\left(-\left(\frac{\frac{\omega}{\omega_p}-1}{\sigma\sqrt{2}}\right)^2\right) \tag{21}$$

where

H_s = the significant wave height

T_p = the peak period corresponding to the frequency ω_p with the highest energy density

γ = 3.3 (peakedness factor)

σ = a step function of ω: if $\omega \le \omega_p$ then: $\sigma = 0.07$
a step function of ω: if $\omega > \omega_p$ then: $\sigma = 0.09$

By applying linear superposition of the body responses, expression for the power absorption in irregular waves can be obtained as:

$$P_{abs,irr} = \int_0^\infty c_{pto}\omega^2\left(\frac{z_A}{\zeta}\right)^2 S(\omega)d\omega \tag{22}$$

where c_{pto} is the linear PTO damping coefficient, z_A is the oscillation amplitude in the frequency domain, ζ is the wave amplitude and $S(\omega)$ is the wave spectrum. A wave with 2.5 m height and a period of 8 s was chosen, based on the moderate wave climate at Chabahar Bay.

Fig. 20 shows the relationship between H_S' and the trend of PTO damping coefficient (c_{pto}) in irregular waves. From this Figure, it can be seen that by increasing the significant wave height, the optimal PTO damping coefficient of the system will increase.

Also, the performance test in irregular wave condition has been carried out for the system. The optimal damping condition was applied to an input of irregular wave spectrum that was generated with $H_s = 2.5$ m and $T_p = 8$ s. Using the wave profile, the simulations were performed in time domain. Fig. 21 shows the motion responses of the floating body and submerged body. Fig. 22 shows the instantaneous absorbed power for the two-body WEC system in irregular wave. One can see that the instantaneous absorbed power remains within the range between 0 and 440 W. As shown in Fig. 22, the average power produced by the system is determined, approximately, 98 kW.

VI. CONCLUSION

In this study, the floating-point absorber wave energy converter system was evaluated with two degrees of freedom. The nonlinear equations for calculating the dynamic response of a two-body WEC, which oscillates in the heave or vertical motion, are solved. The two-body WEC comprises a floating body, an oscillating point-absorber, and a submerged body which is connected to a PTO system. The PTO system was modeled as a spring and damper system. Therefore, the effects of PTO damping and effective parameters were examined and optimized in order to maximize the output power. Considering the resonant frequency of 0.125 Hz as the frequency of the system in all cases, there will be maximum system efficiency. This study has illustrated the application of a hydraulic power take off (PTO) system. To this end, hydraulic simulation model was used and the behavior of a point absorber WEC was examined with a hydraulic PTO. In order to obtain the resonance condition and the maximum power of the system, the values of the hydraulic parameters were determined based on optimal PTO coefficients.

The results indicated that the maximum hydraulic output power is obtained when the generator damping coefficient is 5.21 N · m/(rad/s), which occurs at frequency of 0.125 Hz ($T = 8$ s). This value is calculated by considering the damping in the cylinder and the drop in the pressure system. The value obtained for this coefficient can provide conditions for an optimal PTO damping coefficient (c_{pto}) of 1200 in the system. The results also revealed that by choosing the piston area, motor displacement, and generator damping values within the specified ranges, a remarkable increase of the power absorption efficiency in the PTO system is achieved. moreover, in order to maintain the required motor speed, motor displacement is continuously varying. However, the motor speed should be remained within the operational limits for the PTO system in various wave conditions.

Based on the PTO damping configuration, it can be observed that, the optimal PTO damping values in a wave climate are different from the values for regular waves. The performance test in irregular wave has been carried out for the system and the systems were designed for a nominal irregular sea state with a significant height of 2.5 meters and the peak period of 8 s. In this sea state, the average power produced by the system is approximately 98 kW.

REFERENCES

Alamian, R., R. Shafaghat, S. Jalal Miri, N. Yazdanshenas and M. Shakeri (2014). Evaluation of technologies for harvesting wave energy in Caspian Sea. Renewable and Sustainable Energy Reviews 32, 468-476.

Amiri, A., R. Panahi and S. Radfar (2016). Parametric study of two body floating point wave absorber. J. Marine Sci. Appl. 15, 41-49.

Bozzi, S., A. M. Miquel, A. Antonini, G. Passoni and R. Archetti (2013). Modeling of a point absorber for energy conversion in Italian Seas. Energies 2013(6), 3033-3051.

Brooke, J (2012). Wave Energy Conversion, Elsevier Ocean Enigneering Series, Volume 6, USA.

Cargo, C. (2012). design and control of hydraulic power take-offs for wave. energy converters. PHD. Thesis, Department of Mechanical Engineering, University of Bath, England.

Casey, S. (2014). Modeling, simulation, and analysis of two hydraulic power take-off systems for wave energy conversion. Master of Science thesis, Head of the School of Mechanical, Industrial & Manufacturing Engineering, Oregon State University, USA.

Faizal, M., M. Rafiuddin Ahmad and Y. H. Lee (2014). A design outline for floating point absorber wave energy converters. Advances in Mechanical Engineering 6, 846097.

Falcao, F. de O. (2010). Recent wave energy utilization: a review of the thechnologies. Renewable and Sustainable Energy Reviews 14, 899-918.

Finnegan, W. and J. Googins (2012). The structural dynamics of a two-body wave energy converter. 4th International Conference on Ocean Energy, 17 October, Dublin, Ireland.

Kalofotias, F. (2016). Study for the hull shape of a wave energy converter-point absorber. Master of Science thesis, Water Engineering & Management, University of Twente, Netherlands.

Kassem, A., A. Besheer and A. Abdelaziz (2015). A linear Quadratic Gussian Approach for power transfer maximization of a point absorber wave energy converter. Renewable Energy Devices and Systems 43(8-10), 1173-1181.

Koh, H. J., W. S. Ruy, H. Cho and H. M. Kweon (2015). Multi-objective Optimum design of a buoy for the resonant-type wave energy converter. Journal of Marine Science and Technology 20(1), 53-63.

Kurniawan, A. (2013). Modelling and geometry optimization of wave energy converters. PHD. Thesis, Faculty of Engineering Science and Technology, Department of Marine Technology, Norwegian University of Science and Technology, Norway.

Khojasteh, D. and R. Kamali (2016). Evaluation of wave energy absorption by heaving point absorbers at various hot spots in Iran seas. Energy 109, 629-640.

Liang, C. H. and L. Zuo (2017). On the dynamics and design of a two-body wave energy converter. Renewable Energy 101, 265-274.

Li, Y. and Y. Yu (2012). A synthesis of numerical methods for modeling wave energy converter-point absorbers. Renewable and Sustainable Energy Reviews 16(6), 4352-4364.

Nazari, M., H. Ghassemi, M. Ghiasi and M. Sayehbani (2013). Design of the point absorber wave energy converter for assaluyeh port. 10th International Energy Conference, Islamic Republic of Iran.

Pastor, J. and Y. Liu (2014). Power absorption modeling and optimization of a point absorbing wave energy converter using numerical method. Journal of Energy Resources Technology 136(2), 021207.

Ports and Maritime Organization of Iran: http://www.pmo.ir

Rashid, A. and S. Hasanzadeh (2011). Status and potentials of offshore wave energy resources in Chahbahar area (NW Omman Sea). Renewable and Sustainable Energy Reviews 15, 4876-4883.

Xie, J. and L. Zuo (2013). Dynamics and control of ocean wave energy converters of wave energy converters 1(3), 262-276.

Yu, Y. H and Y. Li (2013). Rynolds-Averaged Navier-Stokes simulation of the heave performance of a two-body floating-point absorber wave energy system. Computers & Fluids 73(15), 104-114.

Yu, Y. H. and Y. Li (2011). A RANS simulation of the heave response of a two-body floating-point wave absorber. 21st International Offshore (Ocean) and Polar Engineering Conference, United States.